

QCD critical point: recent developments

Mikhail Stephanov^{1,2,*}

¹Department of Physics, University of Illinois, Chicago, Illinois 60607, USA

²Kadanoff Center for Theoretical Physics, University of Chicago, Chicago, Illinois 60637, USA

Abstract. Recent developments aimed at mapping QCD phase diagram and the search for the QCD critical point in heavy-ion collisions are briefly reviewed.

1 Introduction

Mapping the phase diagram of QCD is a fascinating theoretical challenge with experimental implications ranging from the early Universe to neutron stars and to heavy-ion collision experiments. This report focuses on the recent developments in the search for the QCD critical point – the point where the crossover at low baryon chemical potential becomes the first-order phase transition separating the hadron gas and the quark-gluon plasma phases of QCD. The search for the critical point is a major component of the heavy-ion collision experiments at RHIC [1, 2] (see Fig. 1). A comprehensive theoretical understanding of critical point physics and its manifestations in heavy-ion collisions is crucial for the success of the search. Such a theory effort is underway, as reviewed, e.g., in [3, 4].

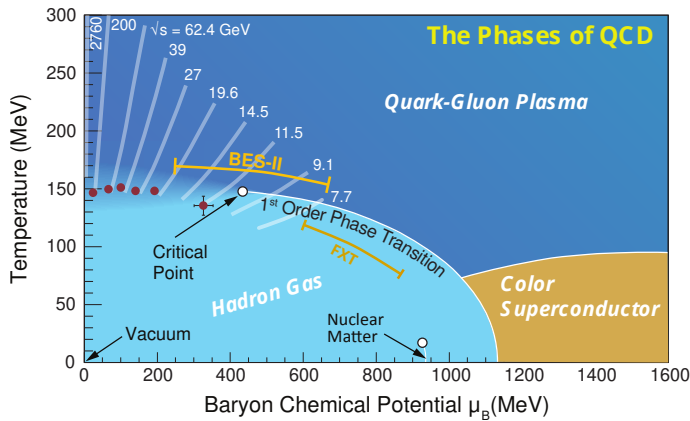


Figure 1. QCD phase diagram and beam energy scan experiments, Ref.[4].

*e-mail: misha@uic.edu

Determination of the location of the critical point by a first-principles theoretical calculation is a longstanding challenge due to the well-known sign problem in lattice Monte Carlo simulations at *finite* μ_B . The most recent results on this front have been obtained by using a broad range of theoretical techniques: Padé resummations of the Taylor expansion in μ_B , whose coefficients are calculated on the lattice [5], also using conformal maps [6], the hybrid lattice plus gauge-gravity correspondence approach (black-hole engineering) [7] and the functional renormalization group approach [8]. These are different methods with different potential sources of systematic errors. It is, therefore, notable, that they all point to the existence of the critical point in the same region of the QCD phase diagram: $T_c \sim 100 - 110$ MeV and $\mu_c \sim 420 - 650$ MeV.

2 Expected signatures and BES-II results

At a recent CPOD 2024 meeting in Berkeley, the STAR collaboration at RHIC presented the results of the latest beam energy scan (BES-II) experiment [9]. The experiment explored the region of the phase diagram marked BES-II in Figure 1 (where the collision energies \sqrt{s} and corresponding fireball expansion histories are also indicated). To appreciate the significance of these results it is helpful to recall the expected signatures of the critical point, see e.g., review [3]. Figure 2 illustrates the expected contribution of the critical point to the baryon density susceptibility (left column), reflecting the QCD equation of state, and to the factorial cumulants of the proton multiplicity fluctuations (middle column), measured experimentally. While the approximate proportionality relationship between the order $n = 2$ (Gaussian) cumulants of these quantities has been known previously, a similar relationship for higher order cumulants ($n = 3$ and 4) has been established recently via the maximum entropy method in Ref.[10], summarized in Section 6.

The purpose of Figure 2 is to highlight the expected *qualitative* features of the *non-monotonic* dependence of these quantities on the collision energy \sqrt{s} . In summary: one expects a peak (or bump) in the 2nd and 3rd cumulants and a dip followed by a peak in the 4th cumulant as μ_B is increased, i.e., \sqrt{s} is *decreased* [3].

The quantitative characteristics of these non-monotonic features — such as the position, height, and width of the peaks — are sensitively dependent on the quantitative properties of the QCD equation of state near the critical point — such as the location, strength and shape of the critical point singularity. While qualitative features of this singularity are universal, the quantitative properties can be described in terms of the non-universal parameters introduced in Ref.[12], see Section 3. The sensitivity to these unknown parameters makes it difficult to predict the critical point signatures quantitatively [13]. Conversely, observation of such signatures would allow us to determine or tightly constrain these important parameters of the QCD equation of state, which is the goal of the experiments.

While quantitative comparison to experimental data has to wait for more quantitative theoretical calculations taking into account not only the equilibrium expectations, but also important non-equilibrium effects, it might still be helpful to analyze the qualitative features of the recent experimental results shown in the *right* column of Figure 2 from the prospective of the equilibrium theory expectations (the *middle* column):

- (1) The apparent dominant feature of the measured $n = 2$ cumulant is its monotonic decrease towards lower \sqrt{s} (increasing μ_B). This effect has been already observed in BES-I data and attributed to baryon number conservation (see, e.g., Ref.[11]). What is notable is that this monotonic decrease is interrupted at lower collision energies $\sqrt{s} \lesssim 11$ GeV. Remarkably such an *excess* over the baseline would be consistent with the presence of the critical point as shown in the sketch for ω_2 in the middle column.

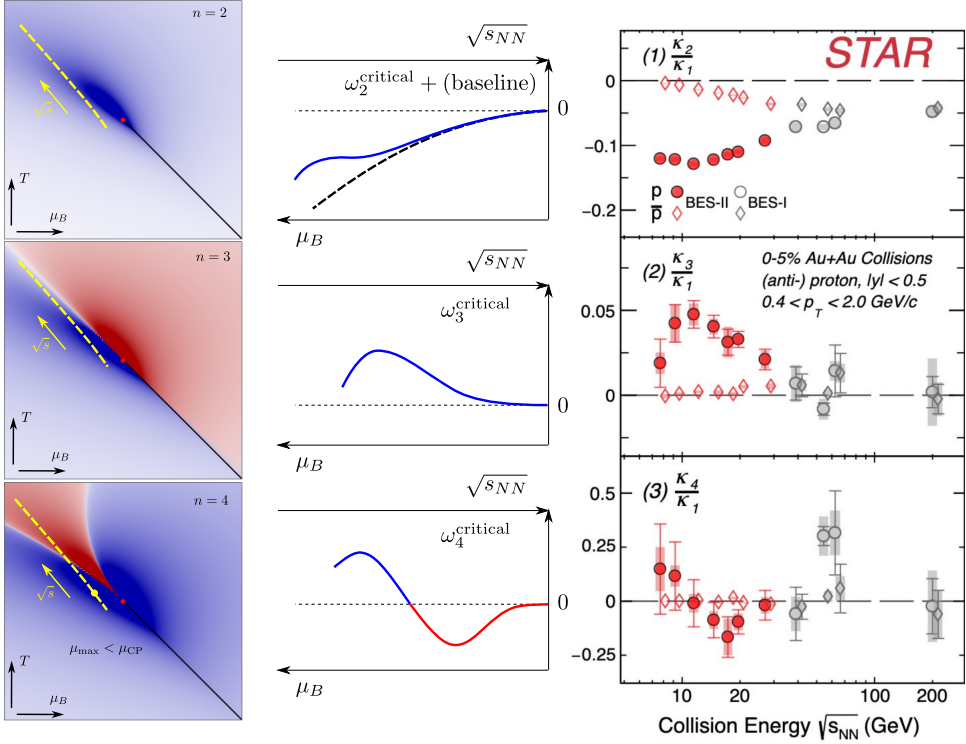


Figure 2. The signatures of the critical point expected in experimentally measured factorial cumulants of proton multiplicity. Each row in the *left column* shows a sketch of the QCD phase diagram region near the critical point (red circle) with the density plot of the baryon density cumulant/susceptibility χ_n for $n = 2, 3, 4$ [3]. The cumulants are positive/negative in the blue/red regions. The yellow dashed line is the freezeout trajectory – a set of points where the heavy-ion collision fireball freezes out as a function of the collision energy \sqrt{s} (as \sqrt{s} increases in the direction of the arrow). The yellow circle marks the point where the cumulant reaches maximum value. The *middle column* shows qualitatively the corresponding expectation for the collision energy dependence of the corresponding (normalized) factorial cumulant of the proton multiplicity $\omega_n \equiv \kappa_n/\kappa_1$ due to the critical fluctuations. For $n = 2$ also the noncritical baseline (evident in the experimental data from BES-I and understood as the consequence of baryon number conservation [11]) is added. The *right column* shows experimental results from BES-II at RHIC reported by STAR [9].

- (2) The dominant feature of the measured $n = 3$ factorial cumulant is the *peak* at around $\sqrt{s} = 11$ GeV. This feature is also in apparent qualitative agreement with the equilibrium expectations for ω_3 shown in the middle column.
- (3) The dominant feature of the $n = 4$ factorial cumulant data is the *dip* at $\sqrt{s} \approx 19$ GeV. This feature also appears to be in qualitative agreement with the equilibrium critical point predictions (middle column) [3, 14, 15]. However, to establish the *peak* feature expected from the critical point at lower \sqrt{s} , the data at $\sqrt{s} < 7.7$ GeV would be necessary. Such data could be provided by the fixed target (FXT) component of BES-II (see Fig. 1) and/or future dedicated experiments.

One must keep in mind that the *non-critical* baseline should be established in order to reach definitive conclusions about the origin of the apparent features of the data, such as, e.g., the peak in ω_3 or the dip in ω_4 .¹ In this regard, the non-monotonicity is a key property of critical fluctuations, which distinguishes them from the monotonic baseline contributions.

It is important to highlight that the critical point on the phase diagram is located at a higher chemical potential μ_B compared to the position of the maximum for each of the cumulants: $\mu_{CP} > \mu_{max}$, as indicated in Fig. 2, left column. Therefore, if the features of the experimental data discussed above are due to the critical point, this critical point has to be located at higher μ_B than 420 MeV — the freezeout point at the lower end of the collision energy range reported in Ref.[9], where the interesting non-monotonic features of the data discussed above appear. Notably, such a critical point location would be also consistent with the recent theoretical estimates [5–8] briefly discussed in Section 1.

It is important to remember that the expectations discussed above are based on the assumption of (local) thermal equilibrium of critical fluctuations. Non-equilibrium effects are important in heavy-ion collisions, of course, and particularly so for determining the critical fluctuation signatures, see e.g., Ref.[16, 17]. The recent developments in describing the non-equilibrium evolution of fluctuations are reviewed in Ref.[4, 18] and, briefly, in Section 5.

The connection between the QCD phase diagram and experimental observables runs through hydrodynamic evolution with a given equation of state, which includes also the evolution of fluctuations, followed by freezeout to convert these hydrodynamic fluctuations into the observable fluctuations of particle multiplicities. The following sections highlight recent advances along this outline.

3 Equation(s) of state of QCD for hydrodynamic calculations

Since the equation of state of QCD in the finite μ_B region where one searches for the critical point is not known, it is necessary to have an efficient parametrization of possible such equations of state, which could then be discriminated by experimental data. Some information about the equation of state is available from lattice calculations, but this information is limited to the region of small μ_B , typically $\mu_B \lesssim 2 - 3T$ by the estimated convergence radius of Taylor expansion. On the other hand, universality of critical singularity constrains the equation of state near the critical point itself up to a few unknown non-universal parameters. Such parameters were introduced and standardized in Ref.[12], where a parametric family of equations of state, which match the lattice data at $\mu_B = 0$ and include a universal critical point singularity, was constructed.

In a more recent work, Ref.[19], a significantly improved parametrization of the QCD equation of state was developed. Its main additional ingredients include the use of the T' expansion scheme, introduced in Ref.[20]. This scheme amounts, essentially, to reorganization of the Taylor expansion in powers of μ_B from being an expansion at fixed T into an expansion at fixed $T'(\mu_B, T)$, where $T'(\mu_B, T) = T_c$ is the equation for the crossover line. In addition, the mapping of T and μ_B on the QCD phase diagram to r and h parameters on the Ising model phase diagram takes into account the C -symmetry $\mu_B \rightarrow -\mu_B$:

$$\frac{T'(\mu_B, T) - T_c}{T'_T T_c} = -hw \frac{\sin(\alpha_1 - \alpha_2)}{\cos \alpha_1}; \quad \frac{\mu_B^2 - \mu_{B,c}^2}{2\mu_{B,c} T_c} = -w(r\rho \cos \alpha_1 + h \cos \alpha_2). \quad (1)$$

where the parameters, introduced in Ref.[12], control the location $(T_c, \mu_{B,c})$, the strength (w) and the shape ($\rho, \alpha_{1,2}$) of the otherwise universal critical point singularity.

¹The various non-critical baselines presented in Ref.[9] fail to adequately explain the data across all collision energies. Generally, the non-critical baselines are monotonic, which prevents them from fully capturing the non-monotonic features of the data.

As a result, the parametric equation of state proposed in Ref.[19] can be used for hydrodynamic calculations in a wider region of the QCD phase diagram, importantly, including μ_B up to 700 MeV, and for a wider range of the critical point parameters.

4 Hydrodynamic trajectories near QCD critical point

Hydrodynamics is a very universal theory which describes a wide range of physical systems from astrophysical, such as neutron stars, to subatomic, such as heavy-ion collisions. Given the equation of state and initial conditions it governs the evolution of hydrodynamic variables – conserved densities characterizing the local (near) equilibrium state of the fluid. Since mapping the QCD phase diagram and determining the equation of state is the goal of heavy-ion collisions, hydrodynamics is the primary tool used to connect the experimental measurements to the underlying QCD equation of state – see Ref.[4] for a recent review.

In order to predict the signatures of the critical point taking into account non-equilibrium effects it is crucial to understand the trajectories on the phase diagram traced by expanding and cooling fireball during its evolution towards freezeout. Under often used, and reasonable, zeroth order approximation of ideal hydrodynamics these trajectories follow the lines of constant specific entropy $\hat{s} \equiv s/n$, where s is the entropy density and n is the baryon density. The singularity of the equation of state near the critical point is responsible for an intricate behavior of these trajectories, which has been understood and classified recently in Ref.[21].

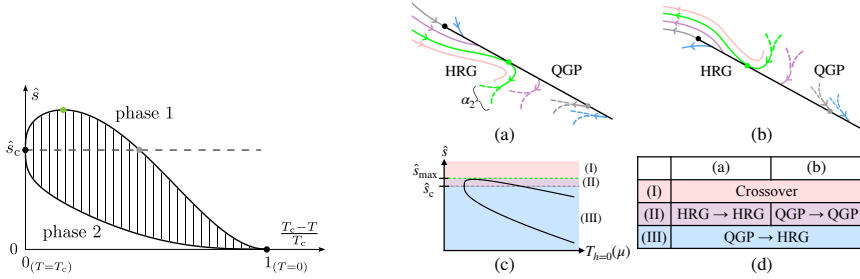


Figure 3. Left: A sketch of the specific entropy as a function of temperature along the phase coexistence line. Right: The classification of isentropic trajectories according to the way they behave in the vicinity of the critical point. See Ref.[21].

The key to this behavior is the non-monotonicity of \hat{s} on one of the branches of the coexistence line (first-order phase transition). The non-monotonicity is a robust consequence of the universality of the singularity at the critical point, which requires \hat{s} to increase away from the critical point, combined with the third law of thermodynamic, which requires \hat{s} to vanish at zero temperature, as illustrated in Fig.3 (left). This gives rise to an interesting pattern of the trajectories near the QCD critical point shown in Fig. 3 (right). The unusual (class II) trajectories enter and reemerge on the *same* side of the coexistence line [21]. Possible experimental consequences of such a behavior are under investigation.

5 Hydrodynamic evolution of fluctuations

In equilibrium, fluctuations of (local) thermodynamic variables are completely determined by equation of state. In particular, the universal singular behavior of fluctuations near a critical point allows us to search for the QCD critical point in experiments. However, hydrodynamic

evolution is characterized by a sustained deviation of the expanding fireball from equilibrium. These deviations are manifested in the departure of the fluctuation measures from their equilibrium values. The evolution of these measures has been a subject of recent research whose progress is reviewed, e.g., in Refs.[4, 18].

A major recent development is the derivation of the deterministic equations for the evolution of the *non-gaussian* fluctuation correlators, which are crucial for the QCD critical point search [22, 23].

Fluctuations are characterized locally by the n -point correlators $H_n \equiv \langle \delta\psi(x_1) \dots \delta\psi(x_n) \rangle$ of hydrodynamic variables, ψ . The evolution equations for these correlators can be derived from stochastic hydrodynamics. The equations can be expanded in and organized by the powers of the small parameter of hydrodynamics – the ratio of the microscopic and hydrodynamic scales – which controls the smallness of the fluctuations. In the diagrammatic representation introduced in Ref.[22] this is a loop expansion. The lowest order, tree level equations were derived in Ref.[22]. Loop corrections lead to the renormalization of hydrodynamic parameters and the so-called “long-time tails”.

The quantities particularly suited for writing and solving fluctuation equations are the Wigner transforms of the correlators H_n , which require a generalization of the well-known two-point Wigner transform to $n > 2$ -point correlators. Such a generalization, $W_n(x, \mathbf{q}_1 \dots \mathbf{q}_n)$, was introduced in Ref.[22]. Physically, W_n describes the magnitude of the correlations of fluctuations with wave-vectors $\mathbf{q}_1, \dots \mathbf{q}_n$ (in the local rest frame of the fluid at point x).

6 Freezeout and maximum entropy

The correlators of hydrodynamic fluctuations $H_n = \langle \delta\psi(x_1) \dots \delta\psi(x_n) \rangle$ discussed in the previous section cannot be measured directly. Instead, experiments measure the correlators of particle multiplicity fluctuations characterized by the event averages $G_n \equiv \langle \delta f(x_1, \mathbf{p}_1) \dots \delta f(x_n, \mathbf{p}_n) \rangle$ (with space-time variables x integrated over the freezeout surface), where $f(x, \mathbf{p})$ are the particle phase space distribution functions.

The measured particle correlators G_n are related to the hydrodynamic correlators H_n . In particular, certain integrals of the particle correlators over momentum space variables $\mathbf{p}_1 \dots \mathbf{p}_n$ are constrained by local conservation laws (of energy, baryon number, etc.) to be equal to the corresponding hydrodynamic correlators. However, of course, there is not enough information in the conservation law constraints alone to determine the particle correlators G_n from given hydrodynamic correlators H_n .

A solution to this problem has been found recently in Ref.[10] by applying the maximum entropy method (MEM). By requiring the entropy of the resonance gas with given correlators G_n to be maximized under the conservation law constraints one obtains a unique solution.

Such a solution passes several nontrivial checks. In particular, applied to the case $n = 1$ it reproduces the well-known and time-tested Cooper-Frye method of freezeout. For critical fluctuations, the MEM matches the most singular contribution to G_n , induced by fluctuations of the effective critical field σ in an earlier approach [3, 14, 17, 24]. MEM goes further, however, and can describe also subleading and even non-critical contributions to multiplicity fluctuations within the same formalism.

In a nutshell, the key observation from the MEM is that the deviations of the hydrodynamic fluctuations from an uncorrelated ideal resonance gas correspond directly to the *factorial* cumulants of the particle multiplicities.² This observation highlights the importance

²More precisely [10], the MEM matches irreducible relative correlators (IRCs) for particle multiplicities, $\hat{\Delta}G_n$, where lower order correlations are subtracted, to similarly constructed hydrodynamic IRCs, $\hat{\Delta}H_n$. The factorial cumulants, κ_n , up to usually negligible quantum statistics effects, are equal to the phase-space integrals of $\hat{\Delta}G_n$.

of *factorial* cumulants as experimental fluctuation measures since these cumulants are more directly related to the QCD equation of state than the normal cumulants.³

7 Conclusions and outlook

The release of the BES-II data by STAR represents a major step towards uncovering the structure of the QCD phase diagram. It is remarkable that the non-monotonic features of the data are in qualitative agreement with the expectations from equilibrium thermodynamics near the QCD critical point, if one assumes such a point is located at $\mu_B \gtrsim 420$ MeV. Such a location of the critical point would be consistent with recent estimates from various theoretical approaches. A comprehensive quantitative comparison of theory with experimental data necessitates dynamic simulations of heavy-ion collisions, incorporating critical fluctuations, which are currently under development.

This work is supported by the U.S. Department of Energy, Office of Science, Office of Nuclear Physics Award No. DE-FG0201ER41195.

References

- [1] M.M. Aggarwal et al. (STAR), An Experimental Exploration of the QCD Phase Diagram: The Search for the Critical Point and the Onset of De-confinement (2010), **1007**.2613.
- [2] G. Odyniec, RHIC Beam Energy Scan Program: Phase I and II, PoS **CPOD 2013**, 043 (2013). [10.22323/1.185.0043](#)
- [3] A. Bzdak, S. Esumi, V. Koch, J. Liao, M. Stephanov, N. Xu, Mapping the Phases of Quantum Chromodynamics with Beam Energy Scan, Phys. Rept. **853**, 1 (2020), 1906.00936. [10.1016/j.physrep.2020.01.005](#)
- [4] L. Du, A. Sorensen, M. Stephanov, The QCD phase diagram and Beam Energy Scan physics: a theory overview (2024), 2402.10183. [10.1142/S021830132430008X](#)
- [5] D.A. Clarke, P. Dimopoulos, F. Di Renzo, J. Goswami, C. Schmidt, S. Singh, K. Zambello, Searching for the QCD critical endpoint using multi-point Padé approximations (2024), 2405.10196.
- [6] G. Basar, QCD critical point, Lee-Yang edge singularities, and Padé resummations, Phys. Rev. C **110**, 015203 (2024), 2312.06952. [10.1103/PhysRevC.110.015203](#)
- [7] M. Hippert, J. Grefa, T.A. Manning, J. Noronha, J. Noronha-Hostler, I. Portillo Vazquez, C. Ratti, R. Rougemont, M. Trujillo, Bayesian location of the QCD critical point from a holographic perspective (2023), 2309.00579.
- [8] Y. Lu, F. Gao, Y.X. Liu, J.M. Pawłowski, QCD equation of state and thermodynamic observables from computationally minimal Dyson-Schwinger equations, Phys. Rev. D **110**, 014036 (2024), 2310.18383. [10.1103/PhysRevD.110.014036](#)
- [9] A. Pandav (STAR collaboration), plenary talk at CPOD 2024, <https://conferences.lbl.gov/event/1376/contributions/8772/>
- [10] M.S. Pradeep, M. Stephanov, Maximum Entropy Freeze-Out of Hydrodynamic Fluctuations, Phys. Rev. Lett. **130**, 162301 (2023), 2211.09142. [10.1103/PhysRevLett.130.162301](#)

³The importance of factorial cumulants (FC), as compared to normal cumulants (NC), has been understood before [25, 26]. In particular, FCs measure deviations of the fluctuations from a Poisson distribution – the natural baseline for *discrete* variables such as multiplicities. These deviations are due to “genuine” (irreducible) correlations between the particles. Finally, the acceptance dependence of FCs (power scaling with Δy) is much simpler than that of NCs.

- [11] V. Vovchenko, V. Koch, C. Shen, Proton number cumulants and correlation functions in Au-Au collisions at $\sqrt{s_{NN}}=7.7\text{--}200$ GeV from hydrodynamics, *Phys. Rev. C* **105**, 014904 (2022), 2107.00163. [10.1103/PhysRevC.105.014904](https://arxiv.org/abs/10.1103/PhysRevC.105.014904)
- [12] P. Parotto, M. Bluhm, D. Mroczek, M. Nahrgang, J. Noronha-Hostler, K. Rajagopal, C. Ratti, T. Schäfer, M. Stephanov, QCD equation of state matched to lattice data and exhibiting a critical point singularity, *Phys. Rev. C* **101**, 034901 (2020), 1805.05249. [10.1103/PhysRevC.101.034901](https://arxiv.org/abs/10.1103/PhysRevC.101.034901)
- [13] J.M. Kartheim, M.S. Pradeep, K. Rajagopal, M. Stephanov, Y. Yin, Equilibrium expectations for non-Gaussian fluctuations near a QCD critical point, in *21st International Conference on Strangeness in Quark Matter 2024* (2024), 2409.16249
- [14] M.A. Stephanov, On the sign of kurtosis near the QCD critical point, *Phys. Rev. Lett.* **107**, 052301 (2011), 1104.1627. [10.1103/PhysRevLett.107.052301](https://arxiv.org/abs/10.1103/PhysRevLett.107.052301)
- [15] E. Shuryak, Four-nucleon clustering near the QCD critical point: theory versus experiment (2024), 2405.16617.
- [16] S. Mukherjee, R. Venugopalan, Y. Yin, Real time evolution of non-Gaussian cumulants in the QCD critical regime, *Phys. Rev. C* **92**, 034912 (2015), 1506.00645. [10.1103/PhysRevC.92.034912](https://arxiv.org/abs/10.1103/PhysRevC.92.034912)
- [17] M. Pradeep, K. Rajagopal, M. Stephanov, Y. Yin, Freezing out fluctuations in Hydro+ near the QCD critical point, *Phys. Rev. D* **106**, 036017 (2022), 2204.00639. [10.1103/PhysRevD.106.036017](https://arxiv.org/abs/10.1103/PhysRevD.106.036017)
- [18] M. Stephanov, QCD Critical Point and Hydrodynamic Fluctuations in Relativistic Fluids, *Acta Phys. Polon. B* **55**, 5 (2024), 2403.03255. [10.5506/APhysPolB.55.5-A4](https://arxiv.org/abs/10.5506/APhysPolB.55.5-A4)
- [19] M. Kahangirwe, S.A. Bass, E. Bratkovskaya, J. Jahan, P. Moreau, P. Parotto, D. Price, C. Ratti, O. Soloveva, M. Stephanov, Finite density QCD equation of state: Critical point and lattice-based T' expansion, *Phys. Rev. D* **109**, 094046 (2024), 2402.08636. [10.1103/PhysRevD.109.094046](https://arxiv.org/abs/10.1103/PhysRevD.109.094046)
- [20] S. Borsányi, Z. Fodor, J.N. Guenther, R. Kara, S.D. Katz, P. Parotto, A. Pásztor, C. Ratti, K.K. Szabó, Lattice QCD equation of state at finite chemical potential from an alternative expansion scheme, *Phys. Rev. Lett.* **126**, 232001 (2021), 2102.06660. [10.1103/PhysRevLett.126.232001](https://arxiv.org/abs/10.1103/PhysRevLett.126.232001)
- [21] M.S. Pradeep, N. Sogabe, M. Stephanov, H.U. Yee, Nonmonotonic specific entropy on the transition line near the QCD critical point, *Phys. Rev. C* **109**, 064905 (2024), 2402.09519. [10.1103/PhysRevC.109.064905](https://arxiv.org/abs/10.1103/PhysRevC.109.064905)
- [22] X. An, G. Başar, M. Stephanov, H.U. Yee, Evolution of Non-Gaussian Hydrodynamic Fluctuations, *Phys. Rev. Lett.* **127**, 072301 (2021), 2009.10742. [10.1103/PhysRevLett.127.072301](https://arxiv.org/abs/10.1103/PhysRevLett.127.072301)
- [23] X. An, G. Basar, M. Stephanov, H.U. Yee, Non-Gaussian fluctuation dynamics in relativistic fluids, *Phys. Rev. C* **108**, 034910 (2023), 2212.14029. [10.1103/PhysRevC.108.034910](https://arxiv.org/abs/10.1103/PhysRevC.108.034910)
- [24] M.A. Stephanov, Non-Gaussian fluctuations near the QCD critical point, *Phys. Rev. Lett.* **102**, 032301 (2009), 0809.3450. [10.1103/PhysRevLett.102.032301](https://arxiv.org/abs/10.1103/PhysRevLett.102.032301)
- [25] B. Ling, M.A. Stephanov, Acceptance dependence of fluctuation measures near the QCD critical point, *Phys. Rev. C* **93**, 034915 (2016), 1512.09125. [10.1103/PhysRevC.93.034915](https://arxiv.org/abs/10.1103/PhysRevC.93.034915)
- [26] A. Bzdak, V. Koch, N. Strodthoff, Cumulants and correlation functions versus the QCD phase diagram, *Phys. Rev. C* **95**, 054906 (2017), 1607.07375. [10.1103/PhysRevC.95.054906](https://arxiv.org/abs/10.1103/PhysRevC.95.054906)